Check for updates

JGR Oceans

RESEARCH ARTICLE
10.1029/2018JC014776

Special Section:
The Three Major Hurricanes of 2017: Harvey, Irma and Maria

Tropical Cyclone Heat Potential and the Rapid Intensification of Hurricane Harvey in the Texas Bight

Henry Potter[1,2], **Steven F. DiMarco**[1,2], **and Anthony H. Knap**[1,2]

[1]Department of Oceanography, Texas A&M University, College Station, Texas, USA, [2]Geochemical and Environmental Research Group, Texas A&M University, College Station, Texas, USA

Key Points:

- Hurricane Harvey intensified over the shallow water of the Texas Bight despite being a region of low tropical cyclone heat potential
- Peak season, warm, well-mixed shelf water limits sea surface cooling and helps contribute to hurricane intensification
- Tropical cyclone heat potential has limited usefulness in shallow water; therefore, subsurface ocean observations are essential for increasing the accuracy of hurricane intensity forecasts

Correspondence to:
H. Potter,
hpotter@tamu.edu

Citation:
Potter, H., DiMarco, S. F., & Knap, A. H. (2019). Tropical cyclone heat potential and the rapid intensification of Hurricane Harvey in the Texas Bight. *Journal of Geophysical Research: Oceans*, *124*, 2440–2451. https://doi.org/10.1029/2018JC014776

Received 15 NOV 2018
Accepted 10 MAR 2019
Accepted article online 15 MAR 2019
Published online 5 APR 2019

©2019. American Geophysical Union. All Rights Reserved.

Abstract Harvey entered the Gulf of Mexico as a tropical depression on 23 August 2017; two days later it had strengthened to a category 1 hurricane. Over the following 30 hr Harvey rapidly intensified, reaching the Texas Bight as a category 3 storm. This intensification continued while Harvey crossed the shelf, making landfall as a category 4 storm 60 km east of Corpus Christi, TX on 26 August. A hydrographic survey two weeks prior to landfall shows that the tropical cyclone heat potential across the Texas Bight was approximately 35 kJ/cm^2, which is 55 kJ/cm^2 less than the amount of upper ocean heat normally associated with intensification. Combined with buoy, float, and satellite data, we use hydrographic surveys to study the conditions of the Texas Bight that contributed to Harvey's rapid intensification. We find that, at the time of landfall, the Texas Bight was well mixed with very warm water extending from the surface to bottom. As a consequence, mixing induced by Harvey had a small impact on surface temperatures which remained high and supported continued intensification. The results show that tropical cyclone heat potential is not an effective metric for hurricane intensity prediction in shallow water, and illustrate the need for continuous subsurface monitoring in order to improve hurricane forecasts.

Plain Language Summary Hurricanes rely on heat extracted from the upper ocean as their energy source. When the ocean is warm conditions are more favorable and hurricanes are often stronger. Hurricanes also mix the ocean which brings cold water from greater depth and can lead to intensity reduction. Tropical cyclone heat potential is a measure of heat in the upper ocean which is available as an energy source for hurricanes. In shallow water tropical cyclone heat potential is typically low because there is not as much water to store heat; therefore, hurricanes are not expected to intensify over shallow water. In this paper we show that hurricane Harvey did intensify over the shallow water off the Texas coast despite having low heat potential. Using ocean measurements, we found that the reason was because the ocean was very warm from the surface to the seabed. Therefore, when Harvey mixed the ocean very little cold water was brought up from below and the surface remained warm which allowed Harvey to continue to strengthen. Results suggest that tropical cyclone heat potential is ineffective for estimating hurricane strength in shallow water and demonstrates the importance of knowing subsurface temperatures if we want to improve hurricane forecasts.

1. Introduction

Tropical cyclones (TCs) are one of nature's most energetic forces. With their powerful winds, extensive rainfall, and associated storm surge they are a serious threat to coastal communities. From 1851 to 2017 an average 1.75 TCs made landfall in the United States annually, 0.6 per year are major (category 3 or greater; Landsea, 2018). Devastation caused by landfalling TCs vary widely and depends on environmental factors such as location, intensity, size, direction of approach, and tidal stage. To reduce the loss of life from TCs it is necessary for forecasts to be accurate so that public trust is built and residents of threatened regions heed evacuation orders. Commendable progress has been made to TC prediction (e.g., Kossin & DeMaria, 2016) but there is still room for improvement, particularly when it comes to intensity forecasting which have made slower gains than track forecasting (DeMaria et al., 2014). One of the reasons for this is that TC strength is heavily influenced by the structure and temperature of the water column (e.g., Jaimes et al., 2015), and while satellite observations can be relied upon to provide sea surface information, this is not true of the subsurface.

21699291, 2019, 4, Downloaded from https://agupubs.onlinelibrary.wiley.com/doi/10.1029/2018JC014776 by Texas A&M University Libraries Eric Hartnett, Wiley Online Library on [10/07/2025]. See the Terms and Conditions (https://onlinelibrary.wiley.com/terms-and-conditions) on Wiley Online Library for rules of use; OA articles are governed by the applicable Creative Commons License

TCs extract their energy from surface enthalpy fluxes so, by first approximation, intensity is a function of sea surface temperature (SST; Emanuel, 1986). A strong relationship between SST and maximum potential intensity has been many times demonstrated (e.g., DeMaria & Kaplan, 1994). Surface forcing by TC winds create divergent surface currents which mix the upper ocean reducing the SST and subsequently decreasing enthalpy fluxes (e.g., Potter et al., 2017) which can reduce intensity by up to 70% (Schade & Emanuel, 1999) The decrease in SST is greatest when the mixed layer depth is shallow and when the thermocline gradient is sharp (Price, 1981). In the northern hemisphere ocean cooling is often most pronounced on the right side of the storm track. This occurs because clockwise inertial currents are accelerated due to rotation of the wind stress vector; this increases mixing and entrainment (Gonella, 1972). Furthermore, the right-front quadrant has the highest waves (e.g., Collins et al., 2018; Wright et al., 2001) which increase breaking and the injection of momentum; this also increases mixing. When models account for stratification and associated feedback arising from vertical mixing and surface cooling in lieu of SST alone, model performance is improved (e.g., Balaguru et al., 2018). However, it is difficult to account for temperature and the upper ocean thermal structure because relevant observations are lacking. Furthermore, studies that have explored these factors as they relate to TC-ocean interaction (e.g., Huang et al., 2009; Park et al., 2011) tend to focus on the deep ocean while shirking coasts. The unfortunate consequence is that perhaps less is known about TCs in the crucial hours before making landfall than at any other time.

Tropical cyclone heat potential (TCHP)—first introduced by Whitaker (1967) as hurricane heat potential and often referred to as ocean heat content (OHC)—is the vertical integration of ocean temperature above 26 °C. This metric was popularized by Leipper and Volgenau (1972), who recognized that when SST is cooled below the air temperature energy is not readily extracted from the sea and the hurricane can no longer be sustained, writing "The rate at which [surface] temperature decrease occurs determines the change in rate at which energy is fed into the storm." The 26 °C isotherm is used because this was seen as the temperature below which hurricanes do not form (Byers, 1959) and the mean tropical atmospheric temperature during hurricane season (Malkus, 1962). TCHP can be estimated using sea surface height anomaly and integrating the thermal structure to the 26 °C isotherm using historical hydrographic data (Goni et al., 2009). Altimeter-derived TCHP has been used operationally by NOAA's Hurricane Center since 2004 (Mainelli et al., 2008) and produces more accurate forecasts than using SST alone. Mainelli et al. (2008) demonstrated that TCHP >60 kJ/cm^2 increases TC intensity; below this value a slight weakening occurs. Other studies have also linked high TCHP to TC intensification (e.g., Wang et al., 2018). The classic example is that of Hurricane Opal in the Gulf of Mexico (GoM), October 1995 (Shay et al., 2000), which intensified from category 1 to category 4 in 14 hr when it went over a warm-core ring shed from the Loop Current. Inside the ring, warmer temperatures approaching 26 °C extended to 150 m (50 m is common in the GoM); consequently, heat content inside the ring was 113 compared to 63 kJ/cm^2 outside. The Loop Current when intruded is a region of high TCHP (e.g., Jaimes et al., 2016). Currently, NOAA recognizes regions with TCHP above 90 kJ/cm^2, which in the GoM are associated with warm anticyclonic rings shed from the Loop Current, are most likely to cause sudden TC intensification.

TCs spend most of their time over deep ocean basins where they have the potential to encounter regions of high TCHP. In contrast, the continental shelf is relatively shallow. Where Harvey made landfall, the outer edge of the shelf is a little more than 100 m deep and the 50-m isobath is 60 km offshore. At the Texas-Louisiana boarder the shelf is much wider and the 50-m isobath reaches 150 km from the coast. In the shallower parts of the continental shelf, TCHP can become limited not by the depth of the 26 °C isotherm but by the depth of the ocean. For example, in an idealized case, 30 m of uniform 30 °C water would have a TCHP less than 50 kJ/cm^2, which is theoretically unfavorable for intensification (i.e., the ocean heat content should not support storm strengthening). Yet Hurricane Harvey did intensify as it crossed the Texas Bight. For the purposes of this study we define the Texas Bight as the portion of the GoM that extends along the coast between Freeport and Port Isabel, TX, and offshore to the shelf break. Here using an ensemble of observational data, we will demonstrate that, despite having relatively low TCHP, the staggering amount of heat packed into this shallow region provided the energy necessary for Harvey to not only sustain its major hurricane status but also increase in strength before making landfall.

The paper is laid out as follows: section 2 introduces the data sources and collection, results are presented in section 3, a discussion is shared in section 4, and section 5 is reserved for final remarks and conclusion.

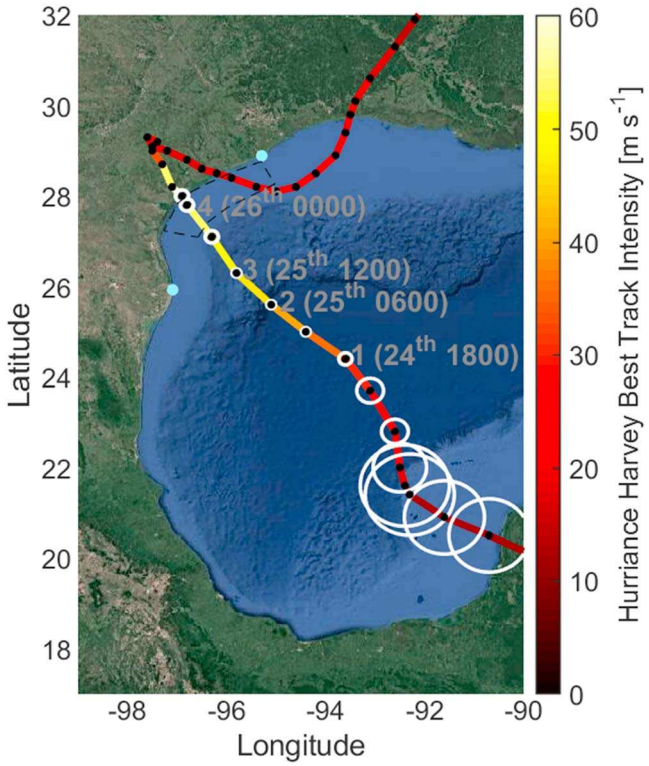

Figure 1. Using extended best track data, Hurricane Harvey best track location, wind speed intensity, and radius of maximum winds. Black dots and white circles show Harvey's location and RMW every 6 hr. The location and time when Harvey reached categories 1–4 status is overlaid in gray type. The area covered by the hydrographic surveys is indicated by the black-dashed polygon. For the purposes of this study we define the Texas Bight as the portion of the GoM from Freeport in the east to Port Isabel in the west (indicated by blue dots) extending offshore to the shelf break.

2. Data

2.1. Hurricane Harvey

Harvey's location, maximum winds, central pressure, and radius of maximum wind (RMW) every 6 hr were downloaded from the National Hurricane Center (NHC) best track data archives (Demuth et al., 2006). Times given by NHC, and throughout this paper, are in UTC. Harvey entered the Gulf of Mexico as a tropical depression with 13-m/s wind speed at 00:00 on 23 August. Forty-two hours later, at 18:00 on 24 August, Harvey had strengthened to a category 1 hurricane with a minimum central pressure of 978 mb and 36-m/s wind speed, and had substantially narrowed its RMW from 170 to 28 km. Over the following 30 hr, Harvey traveled northwest maintaining its tight RMW while undergoing rapid intensification (NHC defines rapid intensification as an increase in the maximum sustained winds of a TC of at least 15.4 m/s over 24 hr). At 18:00 on 25 August Harvey crossed the continental rise and entered the Texas Bight as a category 3 hurricane with 54-m/s wind speed. Over the following 6 hr it continued to intensify, reaching category 4 with 941-mb central pressure and 59-m/s sustained winds at 00:00 26 August. The pressure dropped to 937 mb and wind speed was maintained until Harvey made landfall 3 hr later 60 km east of Corpus Christi, TX. Harvey's track, maximum (1 min sustained) wind speed intensity, category, and RMW are shown in Figure 1.

2.2. Hydrographic Surveys

Hydrographic cruises of the Texas Bight were completed 12–16 June and 7–11 August from the R/V *Manta*. These cruises, which covered any area of approximately 17,000 km^2, were part of a Texas Governors Funds project to study dissolved oxygen on the West Texas Shelf. The latter cruise fortuitously occurred just two weeks prior to Harvey. Each cruise consisted of 28+ conductivity, temperature, and depth casts along cross-shelf lines between Padre Island and East Matagorda, TX. Dissolved oxygen (Sea-Bird SBE-43) and fluorescence and turbidity (WetLABS FLNTU) profiles were also recorded and water samples were collected at every station using a six-bottle rosette. Depths ranged from 13 m along the coast to 106 m offshore. Data were also collected using the Acrobat (www.seasciences.com), a winged conductivity, temperature, and depth housing which is towed behind the ship and piloted as it undulates between the surface and the seabed. The Acrobat was used for several ~30-km cross-shelf transect. Supplemental data recorded by the ship's Scientific Computer System include bulk meteorological parameters and water properties (temperature, conductivity) from the flow-through system.

2.3. Buoy Data

National Buoy Data Center (NDBC; https://www.ndbc.noaa.gov/) and Texas Automated Buoys System (TABS; http://tabs.gerg.tamu.edu) both maintain an array of buoys in the Gulf of Mexico which record bulk meteorological and oceanographic parameters that are made publically available in near real time. TABS is funded by the Texas General Land Office and managed and operated by the Geochemical Environmental Research Group at Texas A&M University (Bender et al., 2007). The data are collected for the primary purpose of aiding oil spill response. NDBC is part of the National Oceanographic and Atmospheric Administration's National Weather Service. NDBC manage a global array of buoys to support the understanding of and predictions to changes in weather, climate, oceans, and coast. Both TABS and NDBC provide quality tested air and water temperature (SST proxy), the parameters of interest here, recorded approximately 4–5 m above and 1–2 m below mean water level, respectively. All TABS buoys are in Texas coastal waters, four (buoys D, J, R, and X) have uninterrupted SST time series for several weeks surrounding Harvey's landfall. Two NDBC buoys (42019 and 42035) are located on the Texas shelf and also have uninterrupted SST time series. Data are provided as 30-min mean values by TABS and 1-hr means by NDBC.

21699291, 2019, 4, Downloaded from https://agupubs.onlinelibrary.wiley.com/doi/10.1029/2018JC014776 by Texas A&M University Libraries Eric Hartnett, Wiley Online Library on [10/07/2025]. See the Terms and Conditions (https://onlinelibrary.wiley.com/terms-and-conditions) on Wiley Online Library for rules of use; OA articles are governed by the applicable Creative Commons License

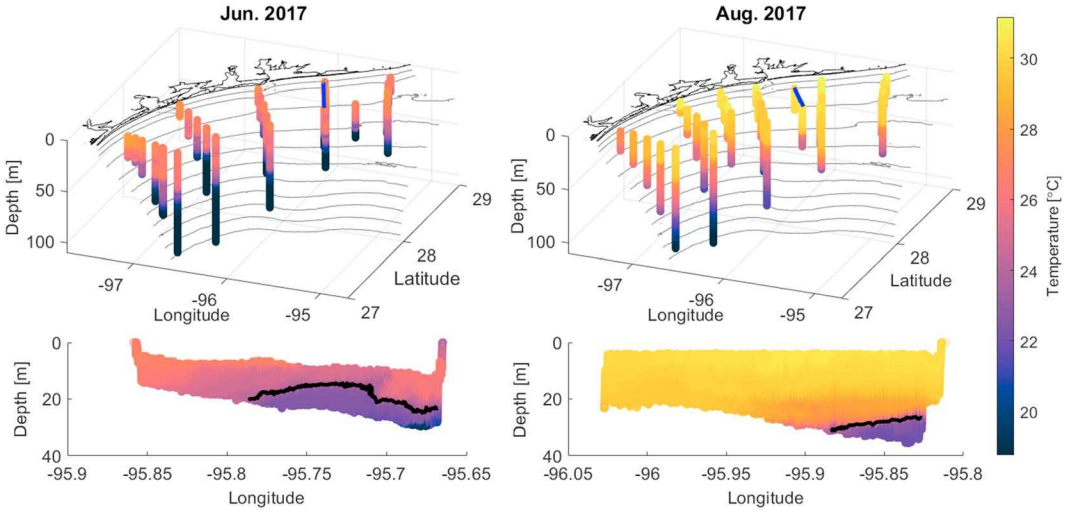

Figure 2. (top) Temperature profiles on the Texas Bight between Padre Island and East Matagorda. The blue lines show the locations of the acrobat tows. (bottom) Temperature recorded during cross-shelf tows with the Acrobat during the June and August cruises. Black lines show the locations of the 26° isotherms.

2.4. Argo Floats

The Argo Program (Argo, 2000), part of the Global Ocean Observing System, consists of a global array of almost 4,000 profiling floats that measure temperature and salinity in the top 2,000 m of the ocean. Data are relayed when the float is at the surface and soon thereafter made freely available by the International Argo Program and the national programs that contribute to it (www.argo.ucsd.edu, argo.jcommops.org). Argo floats spend much of their time neutrally buoyant at depth rising to the surface at approximately 10-day intervals. From 2,000 m it takes about 6 hr to reach the surface during which high-resolution temperature and salinity measurements are made. Fifteen Argo floats were in the western Gulf of Mexico during the nine days (15–23 August) prior to Harvey's arrival; collectively, 21 temperature and salinity profiles were completed.

2.5. Sea Surface Height

Sea surface height anomaly is from Global Analysis Forecast by Copernicus Marine Environmental Monitoring Service (marine.copernicus.eu). Values given are height above geoid with 1/12° horizontal resolution from 24 August.

3. Results

3.1. Hydrographic Surveys

Figure 2 shows the results of the hydrographic surveys. From June to August the water temperatures across the Texas Bight increased markedly. In August the mixed layer was above 30 °C and the average temperature on the shelf was 28.3 °C, 1.8 °C warmer than June. The total heat energy increased from approximately 7.13×10^{13} megajoules (MJ) in June to 7.24×10^{13} MJ in August, a 1.1×10^{12}-MJ change—approximately equal to the estimated electrical energy consumed in the United Kingdom in 2015 (CIA.gov, 2019). The water in August was well mixed with the temperature at the surface extending to the seabed at many locations, especially closer to the coast. This is clearly seen in the Acrobat vertical section data (Figure 2, bottom panels), which illustrates the high August temperatures extending far from the coast. The 26° isotherm, the metric used for TCHP, first appears 47 km from shore. In contrast to August, June temperatures decreased rapidly with depth and the 26° isotherm was shallower and much closer to the coast.

3.2. Sea Surface Temperature

Collectively, six TABS and NDBC buoys moored on the Texas Bight reported water temperature (SST proxy) throughout August 2017. Sensor NDBC 42019 and 42035 were at 1 and 0.6 m, respectively, TABS record temperature between 1.5 and 2 m. Buoy locations are shown in Figure 3 alongside SST from 3 to 28

21699291, 2019, 4, Downloaded from https://agupubs.onlinelibrary.wiley.com/doi/10.1029/2018JC014776 by Texas A&M University Libraries Eric Hartnett, Wiley Online Library on [10/07/2025]. See the Terms and Conditions (https://onlinelibrary.wiley.com/terms-and-conditions) on Wiley Online Library for rules of use; OA articles are governed by the applicable Creative Commons License

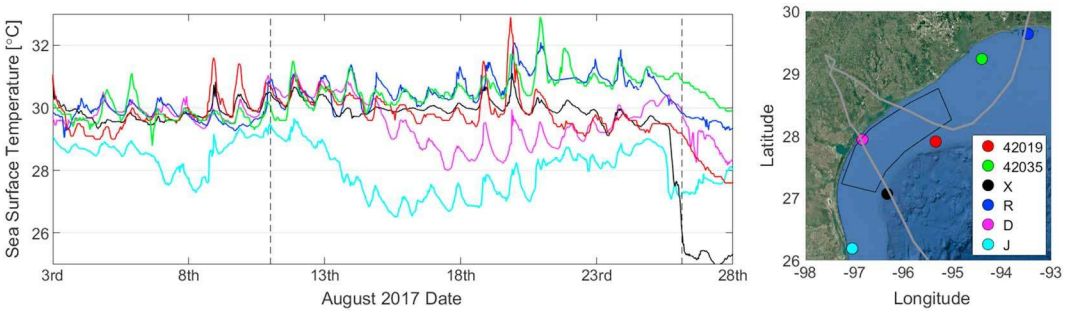

Figure 3. (left) NDBC and TABS August SST in the Texas Bight. From left to right, vertical dotted lines show the dates of the hydrographic cruise and Harvey's landfall. Colors correspond to the buoy locations show on the map. (right) Locations of the buoys. Harvey's track is shown by the gray line and the polygon outlines the hydrographic survey region.

August. These data are plotted here to infer if any significant change in ocean temperature occurred in the two weeks from the August hydrographic survey to Harvey's arrival on the shelf. A brief discussion of the hurricane-induced cooling is provided in section 4.3. All buoys reported the expected diurnal signal and D and J, both along the western coast, showed some longer-term variability. Generally speaking, temperatures decreased marginally at offshore locations but increased along the coast. From east to west, change in foundation temperatures (i.e., free of diurnal increase) between 7 and 11 August (dates of the hydrographic survey) and 25 August (immediately prior to Harvey's landfall) were R: +1.3, 42035: +1.6, 42019: −0.5, X: −0.4, D + 0.4, and J: −0.1. Poststorm the diurnal variability ends and the surface temperature decreases at all buoys near the approaching first landfall storm track.

4. Discussion

4.1. Tropical Cyclone Heat Potential

Tropical cyclone heat potential has been established as an important parameter in TC prediction because it quantifies the heat energy available below the surface rather than relying purely on SST (Leipper & Volgenau, 1972).

$$Q = c_p \sum_{Z_0}^{Z_{26}} \rho_i (T_i - 26) \Delta z_i \quad (1)$$

Q is the TCHP (kJ/cm^2), c_p = 3.85 kJ (kg C)$^{-1}$ is the specific heat of water at a constant pressure, T_i is the water temperature in °C at the ith level, Δz_i is ith layer water thickness (50 cm), and ρ_i is the density of water at the ith level. Z_0 and Z_{26} are the surface and the depth (m) of the 26 °C isotherm. Here we use equation (1) to determine the TCHP in the GoM prior to Harvey on the shelf using hydrographic cruise data and off the shelf using Argo data. Density was recorded during the hydrographic cruises; Argo do not report density so it was calculated from temperature, salinity, and pressure using the 75-term equation available from Gibbs-SeaWater Oceanographic Toolbox (McDougall & Barker, 2011).

The TCHP increased greatly between June and August in the Texas Bight. Mean shelf-wide values were 17 and 35 kJ/cm^2, respectively. Notwithstanding this doubling, TCHP remained markedly below the 90 kJ/cm^2 associated with hurricane intensification. August TCHP was lowest close to shore where it was limited by the depth of the water, not the depth of the 26 °C isotherm. This condition extended 47 km offshore to depths exceeding 30 m, beyond which bottom temperatures dropped below 26 °C. Highest August TCHP was observed at the furthest offshore station for each transect where the 26 °C isotherm was between 30 and 45 m. TCHP for the June and August cruises are shown in Figure 4.

Between the second hydrographic cruise and Harvey the TABS and NDBC buoy data show that the mean SST change across the Texas Bight was +0.4 °C (recall Figure 3). If this temperature increase extended throughout the water column and across the entire study region, TCHP would have increased 5 kJ/cm^2 leaving the Texas Bight well below the threshold associated with TC intensification. Nonetheless, Harvey continued to intensify, transitioning from category 3 to a category 4 TC over 6 hr following its arrival on the shelf. This was a continuation of intensification that started when Harvey

21699291, 2019, 4, Downloaded from https://agupubs.onlinelibrary.wiley.com/doi/10.1029/2018JC014776 by Texas A&M University Libraries Eric Hartnett, Wiley Online Library on [10/07/2025]. See the Terms and Conditions (https://onlinelibrary.wiley.com/terms-and-conditions) on Wiley Online Library for rules of use; OA articles are governed by the applicable Creative Commons License

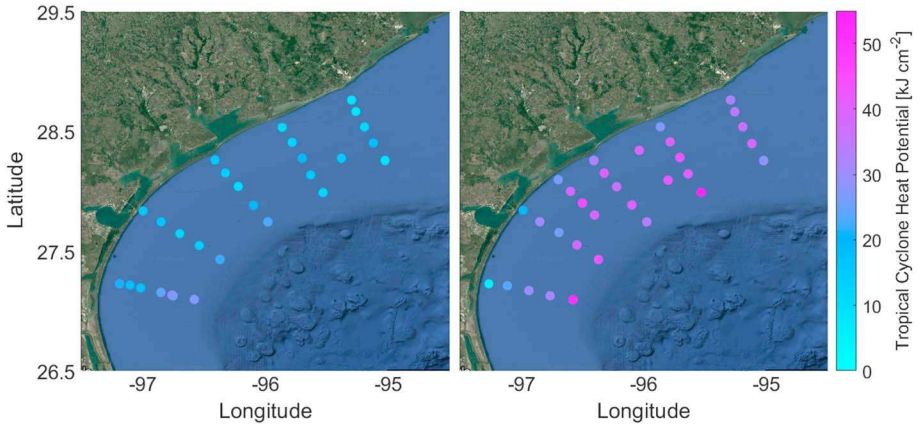

Figure 4. Tropical cyclone heat potential (kJ/cm^2) of the Texas Bight in (left) June and (right) August as determined from conductivity, temperature, and depth casts conducted during repeat hydrographic surveys.

become category 1 on 24 August 18:00 and lasted 30 hr. During that time U_{max} increased 23 m/s, almost twice the rate required for rapid intensification. Before reaching the shelf, Harvey spent the preceding 24 hr in deep water strengthening from category 1 to category 3. Data collected from 14 autonomous profiling floats deployed in the GoM over four years show that heat content in the upper 800 m peaks between August and September and temperature of the top 10 m peaks in August (Hamilton et al., 2018). With respect to intensification, Harvey's arrival was therefore timely. Notwithstanding, Trenberth et al. (2018) suggested that, as a result of climate change, the GoM was extremely warm, whereby it provided increased fuel to sustain and intensify Harvey. Meanwhile, researchers at Louisiana State University Earth Scan Laboratory (Gulf of Mexico Coastal Ocean Observing System Banner Story, 2017) and University of Miami (Becker, 2017) have both suggested that Harvey intensified because it crossed the remnants of a Loop Current eddy with high TCHP.

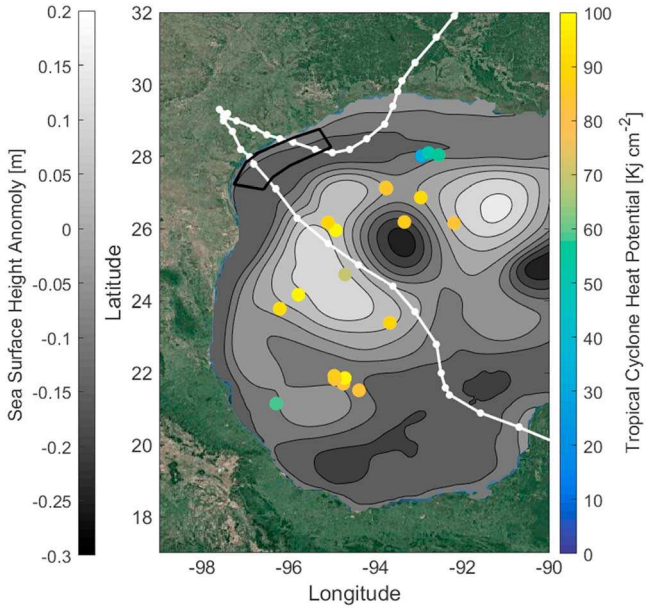

Figure 5. Sea surface height anomaly on 24 August from Copernicus and TCHP as determined from 21 Argo float profiles between 15 and 23 August (dots represent location at time profile was completed, and color depicts TCHP). Contour lines show 5-cm steps. Maximum value of the eddy Harvey passed though was approximately 12 cm. Harvey track and location every 6 h is in white and the polygon marks the outline of the hydrographic survey region. Note that the colors in the TCHP color bar are the same as in Figure 4 but the range has been expanded.

We join in the discussion briefly here using sea surface height anomaly from Copernicus and TCHP determined from Argo float data (Figure 5). The GoM was indeed very warm. Seven Argo profiles reported TCHP above or very close to 90 kJ/cm^2. Five of these were on the outskirts of the eddy approximately bounded by 23–28°N, 93–97°W where sea surface height anomaly was between 5 and 8 cm. The other two were located below geoid (at approximately 21.9°N, 94.7°W and 26.9°N, 93°W). TCHP closest to the eddy's center at 12-cm sea surface height anomaly was only 70 kJ/cm^2. Excluding the four on-shelf profiles, mean TCHP was 87.5 kJ/cm^2. This adds some credence to the theory that 90 kJ/cm^2 is a good indicator that rapid intensification in deep water will occur but does not conclusively show that high TCHP in this case was due to the eddy. Of additional note is that TCHP off the Louisiana coast (north of 28°N, east of 93°W) was 32–54 kJ/cm^2—consistent with far-offshore values determined from the hydrographic survey in the Texas Bight. In both cases, measurements were made on the shelf in approximately 110 m of water.

4.2. Intensification on the Shelf

Harvey entered the shelf as a category 3 hurricane and over the following 6 hr intensified to category 4, U_{max} = 59 m/s at 00:00 26 August (NHC best track). This wind speed was sustained until Harvey made landfall 3 hr later, only then did it began to weaken. During its 9-hr shelf crossing,

21699291, 2019, 4, Downloaded from https://agupubs.onlinelibrary.wiley.com/doi/10.1029/2018JC014776 by Texas A&M University Libraries Eric Hartnett, Wiley Online Library on [10/07/2025]. See the Terms and Conditions (https://onlinelibrary.wiley.com/terms-and-conditions) on Wiley Online Library for rules of use; OA articles are governed by the applicable Creative Commons License

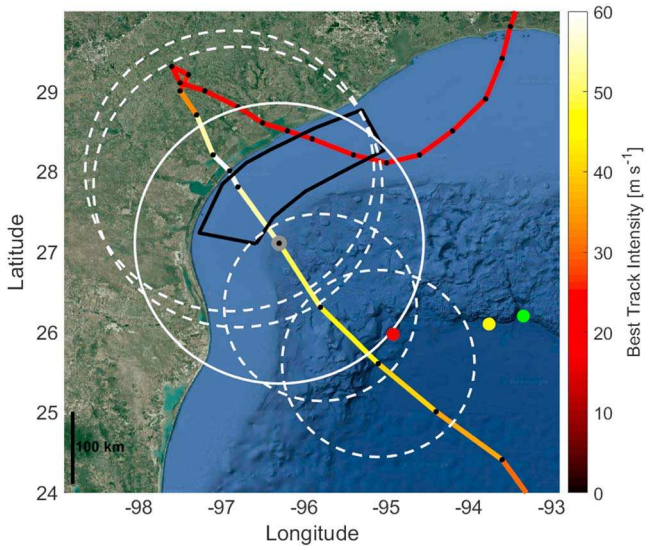

Figure 6. Hurricane Harvey track with best track maximum (1 min sustained) wind speed. Black dots along the track show TC location every 6 hr and white circle surrounding each black dot show 7 RMW (radius of 196 km) at that time. The exception here is the location marker on the coast which is 3 hr removed from the adjacent markers. Large gray dot at the center of the image indicates Harvey's location at 18:00 on 25 August as its eye began to cross the Texas Bight and, in order to differentiate from the others, 7 RMW is plotted as a solid line. NDBC-42002 is located at the yellow dot and Argo floats 4901480 and 4902296 were located at the red and green dots, respectively. The black polygon outlines the region of the hydrographic survey. A length scale is at the bottom left of the figure.

Harvey strengthened and sustained very high wind speeds despite being over water with relatively low TCHP.

TCs rely on enthalpy fluxes as their energy source and can neither develop nor maintain their intensity without latent heat input. These fluxes are largely controlled by latent instability between the sea surface and near-surface air and therefore largest over warm oceanic features (Jaimes et al., 2015). The radial extent from which energy can be harvested to fuel a TC is certainly limited but remains open for debate. Using a coarse resolution model, Chang (1979), for example, demonstrated that a TC with RMW > 30 km would decrease in intensity when SST was reduced by 2 °C within 300 km of the storm center or approximately 8–9 RMW. Xu and Wang (2010) studied surface energy fluxes (sensible and latent heat) using a fully compressible, nonhydrostatic TC model. They found that entropy fluxes under the eyewall provide the greatest contribution to TC intensity and those outside the eyewall, to a radius of 60 km (2–3 RMW), are also important. Miyamoto and Takemi (2010), using an axisymmetric, nonhydrostatic model, determined that the radius within which the sea surface flux of moist enthalpy plays a vital role in determining the intensity of a TC is 7–8 times the RMW. Outside this region the enthalpy flux did not have a positive impact on intensity. Results are clearly mixed, ranging from about 2 to 9 RMW. For Harvey, which crossed the shelf with 28 km RMW, this translates to a range of 56 to 252 km. A liberal 7 RMW (196 km) interpretation is applied to examine Harvey's *flux footprint*, that is, the region within which enthalpy fluxes may have provided energy to the hurricane. This is done to explore the extent to which Harvey, while crossing the Texas Bight, might have been impacted by the higher TCHP water off the shelf. Figure 6 shows Harvey's track and 7 RMW as it approached the coast.

Between 18:00 25 and 00:00 26 August, as it entered and crossed the shelf, Harvey's U_{max} increased from 54 to 59 m/s whereby intensifying to category 4. Between 00:00 and 03:00 (when Harvey made landfall), U_{max} remained 59 m/s. As Harvey's eye entered the shelf, the aforementioned 7 RMW flux footprint that was approximately 35% was over deep, higher TCHP water, 38% over lower TCHP shelf water, and 27% over land. Six hours later, values were approximately 14%, 34%, and 52%, respectively. Despite going through 6 hr of intensification followed by 3 hr with sustained category 4 wind speeds, just one third of the flux footprint, decreasing to less than 10% at landfall, was over the deep ocean. Rerunning the analysis using a conservative 3 RMW (84 km) the values were approximately 46% over the deep Gulf and 54% on the shelf at 18:00 becoming 62% shelf and 38% land by 00:00. While energy from the higher TCHP region off the shelf may have contributed marginally to Harvey's intensification as it approached land (particularly for the 7 RMW case), there is a further reason to believe that any contribution was nominal, namely, the cold wake—a region of cooler SST and reduced upper ocean heat content. Cold wakes are typically most prevalent on the right side of the TC track in the northern hemisphere which induces strong enthalpy flux asymmetry with relatively lower values in the rear-right quadrant (Lee & Chen, 2012). Undoubtedly, Harvey's cold wake reduced TCHP across the GoM and, when crossing the Texas Bight, TCHP in the deep GoM was likely much lower than reported in Figure 5. To quantify this we turn again to NDBC and Argo.

NDBC-40002 is moored at 26.1 N, 93.76 W at the base of the continental rise in 3,125-m water (see Figure 6). Foundation SST at this location was 30.9 °C on 23 August. By 18:00 on 25 August as Harvey entered the Texas Bight, SST had decreased to 30.4 (Figure 7). Applying this 0.5 °C decrease to the profile recorded by the closest Argo float (4902296), which was 43 km east and completed a profile at 07:00 23 August, would raise the 26 °C isotherm from 57.5 to 55.5 m and decrease TCHP from 87 to 75 kJ/cm^2. Although a crude approximation, it is commonplace for category 3 TCs to impact the water to 100 m (Price, 2009), and it nevertheless indicates that when Harvey arrived at the shelf, the off-shelf TCHP was reduced. The only Argo float in the vicinity of the shelf which completed a profile shortly after Harvey was float 4901480 (see Figure 6). This float's pre-Harvey profile was recorded on 18 August when TCHP was 103 kJ/cm^2. The following

21699291, 2019, 4, Downloaded from https://agupubs.onlinelibrary.wiley.com/doi/10.1029/2018JC014776 by Texas A&M University Libraries Eric Hartnett, Wiley Online Library on [10/07/2025]. See the Terms and Conditions (https://onlinelibrary.wiley.com/terms-and-conditions) on Wiley Online Library for rules of use; OA articles are governed by the applicable Creative Commons License

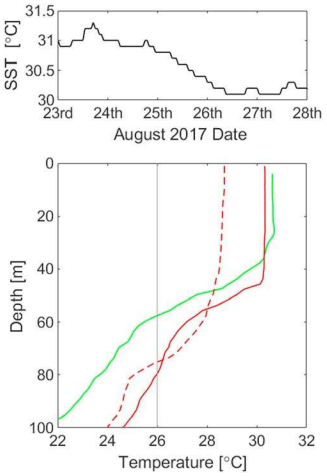

Figure 7. (top) SST at NDBC-42002. (bottom) Argo temperature profiles for float 4902296 on 23 August 23 (green) and float 4901480 on 18 August (red) and 28 August (red-dashed). The gray vertical line marks the location of 26 °C isotherm used to determine TCHP.

profile on 28 August showed that extensive cooling had occurred (Figure 7) and TCHP was 69 kJ/cm^2, over 30% reduced. Given the frequency of reporting and the changes in position of the float, there is no way of knowing when this decrease occurred. Notwithstanding, it is likely that much of the heat was displaced before Harvey passed the float, which is typical of TC-induced upper ocean cooling. Potter (2018), for example, showed that a category 4 typhoon with 34 km RMW and 3.6-m/s translation speed V_p, similar to Harvey (RMW = 28 km, V_p = 4.2 s), can induce upper ocean cooling two days before passing the measurement site and continue several days after. Since Harvey entered the Bight 12 hr after passing Argo 4901480, a fair deduction is that much, if not all, of the TCHP reduction had occurred by that time.

4.3. Heat Distribution

When it reached category 4, with approximately half of the flux footprint over land and 15% off the shelf, the remaining ~35% on the shelf (in the 7 RMW flux footprint case) must have contributed sizably to Harvey's strength. This is despite lacking the TCHP typically associated with rapid intensification. We suggest that the condition that made this possible was the large amount of heat packed in the relatively narrow region between the surface and the seabed. TC intensification typically occurs when SST is high—so a lot of heat energy is provided to the storm—and when the mixed layer is thick (O 100 m; e.g., Lin et al., 2005). A thick mixed layer restrains the sea surface cooling (cold wake creation) by limiting entrainment across the base of the thermocline allowing continued sea-to-air enthalpy flux which favors intensification (Wang et al., 2018). The same may be said when the ocean is shallow but hot as was the case on the Texas shelf. In the absence of a thermocline water entrained or upwelled, and—to a greater or lesser extent—horizontally advected, was essentially the same temperature as at the surface insomuch that it would provide an environment favorable to Harvey's continued strengthening.

In the week leading up to landfall coastal buoys NDBC 42035 and TABS-R in the northern Texas Bight show surface water increased to ~31 °C and was the warmest region on the shelf (recall Figure 3). The August hydrographic cruise also shows that the warmest SST resided in the northern extent of the survey. When Harvey approached land, TABS indicate that currents were downcoast (DiMarco et al., 2018) so this warm water was advected toward Harvey's eye region. Jaimes et al. (2016) found that nonlinear interaction of wind stress and geostrophic flow under tropical storm Isaac (2012), as it passed between two warm-core eddies in the GoM, produced a horizontal convergence of warm water. This surface warming enhanced enthalpy fluxes as Isaac intensified into a category 1 hurricane. It is plausible that similar conditions occurred as Harvey cross the shelf which contributed in some capacity to its intensification. Unfortunately, few studies have focused on the ocean under landfalling hurricanes so the extent to which warm water channeled along coast toward the storm contributes to its strength is unknown. However, some notable research by Shen and Ginis (2001) determined that, at landfall, so long as ocean depth is “much greater” than the mixed layer, cold wake behind the storm acts to reduce the near-surface entropy advection into the hurricane core. In doing so, the energy source is reduced as with a deep-ocean storm. For Harvey which crossed a wide shelf, this was not the case and the limited cooling is thought to have sustained the air-sea enthalpy flux.

To better understand heat on the shelf, Figure 8 shows the depth difference δz (m) between the seabed and the 26 °C isotherm (if there is one). For half the stations $\delta z = 0$, that is, the bottom temperature was above 26 °C, these were concentrated in the north and east of the shelf study region. Further south and offshore δz increases marginally, five locations had $0 < \delta z \leq 10$ and six had $10 < \delta z \leq 20$. Only four locations had $\delta z > 20$. A consequence of having a narrow region of sub-26 °C water near the seabed is that in all but three cases where $\delta z > 0$ (namely, the easternmost stations on transects 4, 6, and 7, counting from north to south) mean water column temperature was above 26 °C. Indeed, values in the realm of 28 °C were more typical, which meant that even a complete mixing of the water column would not substantially decrease the surface temperature. This is well illustrated in Figure 3. TABS-D, located in a region with $\delta z = 0$, showed no decrease in SST until several hours after Harvey made landfall. The same was true of NDBC-42035. At the edge of

21699291, 2019, 4, Downloaded from https://agupubs.onlinelibrary.wiley.com/doi/10.1029/2018JC014776 by Texas A&M University Libraries Eric Hartnett, Wiley Online Library on [10/07/2025]. See the Terms and Conditions (https://onlinelibrary.wiley.com/terms-and-conditions) on Wiley Online Library for rules of use; OA articles are governed by the applicable Creative Commons License

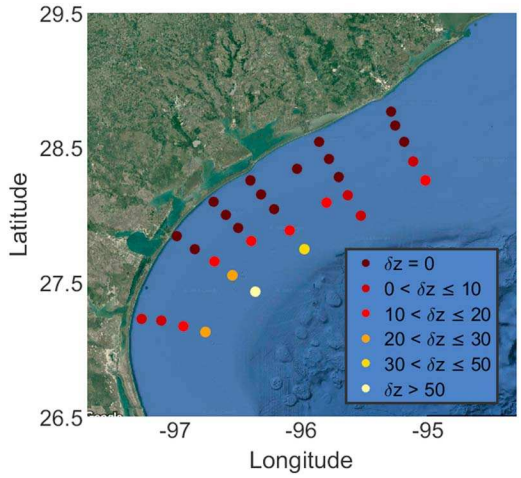

Figure 8. Depth difference δz in meters between the 26 °C isotherm and the seabed in August 2017. Where the bottom temperature exceeds 26 °C, δz = 0.

the shelf, NDBC-42019 (δz ≈ 9.5 m) recorded a more noticeable, if marginal, decrease by landfall but remained above 29 °C, whereas TABS-X (δz ≈ 23 m) reported an abrupt SST drop of ~4 °C, half of this occurred after landfall. Indeed, at the time of landfall SST across the shelf remained high, acting to sustain Harvey's intensification. Save TABS-X and J where cooling was abrupt, the slow, steady temperature decrease at the other buoys is believed to be caused by precipitation and the lingering effect of Ekman pumping and internal wave breaking which continued to move water laterally and vertically. A more involved analysis of the impact of Harvey on Texas coastal waters is beyond the scope of this analysis but is forthcoming in a related manuscript.

An examination of the air temperature revealed a great deal of variability. Of the NDBC and TABS buoys in the region, four reported values from 18:00 25 to 00:00 26 August. These ranged from 23 to 29 °C and were very mercurial—as one might expect given the circumstances. They reveal no clear spatial pattern but nonetheless show that air temperature was generally below SST, supporting sea-to-air energy heat flux and reinforcing the assertion that conditions were favorable to TC growth.

5. Final Remarks and Conclusion

TC intensification in the Texas Bight is not unique to Harvey. Of the 13 other named storms that crossed the shelf since 1995 five intensified. Dean (1995), Charlie (1998), and Bill (2015) were tropical storms, while Claudette (2003) and Humberto (2007) were both hurricanes. Humberto, most notably, intensified from 23 to 41 m/s over 12 hr on 13 September. At that time, SST along the Texas coast was at the annual peak, which typically extends from early August to mid-September (TABS, NDBC; data not shown). While high SST likely contributed to Humberto's intensification, the data do not suggest that peak season SST is a precursor to intensification in the Texas Bight. Of the five aforementioned storms, three occurred between early August and mid-September, and of the remaining eight, five crossed the shelf during this period without intensifying. In addition to the heat of the underlying ocean, there are several environmental factors which are known to be indicative of stronger storms and intensification. These include eyewall replacement, storm translation speed, storm size, and wind shear. While it is beyond the scope of this paper to compare and contrast these factors as they apply to the aforementioned storms—and potentially uncover the mechanisms of their intensification—below we briefly discuss each as it pertains to Harvey.

Storm translation speed: Mei et al. (2012) showed that slow-moving storms have more time to be impacted by sea surface cooling which enhances the negative feedback on storm intensity. Lin et al. (2009) found fast-moving storms (~7–8 m/s) can have sufficient enthalpy flux to intensify to category 5 even when over relatively low TCHP water (65–70 kJ/cm^2). Harvey's translation speed, 5.2 m/s approaching the shelf and 4.2 m/s crossing the shelf, was much slower and at a rate more typical of self-debilitation through surface cooling. Eyewall replacement: Eyewall replacements cycles go through three stages: intensification, weakening, and reintensification (Sitkowski et al., 2011). The result is that on average hurricanes contract 12 km and intensify 2 m/s. NOAA's Hurricane Harvey Tropical Cyclone Report (Blake & Zelinsky, 2018) does not report Harvey went through an eyewall replacements cycles. Nonetheless, the possibility of an eyewall replacements cycles contributing incrementally to Harvey's intensity cannot be discounted. Tropical cyclone size: The relationship between strength, intensity, and size (with multiple nuanced definitions of each) is somewhat complex. Nonetheless, clear evidence of a relationship between TC size and intensity is lacking. Carrasco et al. (2014) found little or no correlation between radius of the last closed isobar (RLCI) and intensity. Weatherford and Gray (1988) showed that by itself eye size does not have much of a relationship with mean minimum sea level pressure but a contracting eye is on average associated with a minimum sea level pressure decrease. Similarly, Carrasco et al. (2014) determined that RMW has a negative correlation with change in intensity but the RLCI has little or no relationship with intensification. Prior to entering the shelf Harvey's RMW increased and RLCI decreased (RMW = 19 km, RLCI = 389 km at 12:00 25 August; RMW = 28 km, RLCI = 333 km at 18:00 25 August). Previous research does not support the idea that this would have affected intensity. Wind Shear: Wind

21699291, 2019, 4, Downloaded from https://agupubs.onlinelibrary.wiley.com/doi/10.1029/2018JC014776 by Texas A&M University Libraries Eric Hartnett, Wiley Online Library on [10/07/2025]. See the Terms and Conditions (https://onlinelibrary.wiley.com/terms-and-conditions) on Wiley Online Library for rules of use; OA articles are governed by the applicable Creative Commons License

shear decreases intensity; as shear increases so does the magnitude of weakening (e.g., Frank & Ritchie, 2001; Weisman & Klemp, 1982). NOAA's Hurricane Harvey Tropical Cyclone Report (Blake & Zelinsky, 2018) does not indicate that Harvey was recovering from wind shear disruption anytime on the approach or over the Texas Bight.

Much remains unknown about the conditions below the sea surface in hurricanes that contribute to their intensification. Harvey caught many people and first response agencies off guard with unexpected rapid intensification. Across the deep water of the GoM rapid intensification may be explained by the high TCHP, the same cannot be said for the shelf where TCHP remains comparatively low because it is limited by the water depth not the depth of the 26 °C isotherm. Even when applying a liberal 7 RMW threshold to estimate the area under which enthalpy fluxes contributed to Harvey's intensity, as it crossed the shelf maximum 10–15% of this flux footprint was over the deep GoM. This means that Harvey must have relied heavily on shelf water to continue intensifying. Hydrographic profiles preceding Harvey and moored buoys (NDBC and TABS) together show that shelf water warmed markedly between June and August and Harvey arrived around peak season for northern GoM temperature. At that time the shelf was packed with heat and mean TCHP was 35 kJ/cm^2, which is well below the value typically associated with intensification. Very warm water extended from the surface to the seabed and the 26 °C isotherm (the metric used to calculate TCHP) did not appear until almost 50 km from the coast in many locations. Further offshore, the vertical extent of sub-26 °C water was marginal such that a complete mixing of the water column would reduce the SST by a few degrees or less. TABS and NDBC SST data indicate that SST did indeed only drop slightly, whereby maintaining conditions favorable to TC intensification.

The threshold to maintain a TC is between about 10 and 16 kJ/cm^2 per day (Leipper & Volgenau, 1972; Shay, 2006), far below typical TCHP values in the subtropical ocean. So why does TCHP below 60 kJ/cm^2 lead to TC weakening (Mainelli et al., 2008), and why are values above 90 kJ/cm^2 associated with intensification? The answer Mainelli proposed is that it is not the extra heat that causes intensification, but the limited SST cooling. When a TC crosses a region with high TCHP and a deep 26 °C isotherm, the mixing of cool subsurface water and subsequent decrease in SST is limited meaning enthalpy fluxes are only nominally reduced and intensity is sustained. The same reasoning can be applied to Harvey when it crossed the shelf. High temperatures extending to the seabed meant mixing minimally decreased SST allowing Harvey's continued intensification. The conditions on the shelf add credence to the recommendation by Price (2009) that depth-averaged temperature $T_{\overline{d}}$ should be used as an alternative to OHC. $T_{\overline{d}}$ provides information about the potential for cooling directly below a TC and the minimum potential SST—which directly impacts intensity—that is not given by OHC. Price (2009) recognized that OHC on the shelf will generally be comparatively low regardless of the ocean temperature, whereas $T_{\overline{d}}$ can have high values, especially where water is warm with neutral or downwelling favorable conditions. This was certainly the case during Harvey and supports the use of $T_{\overline{d}}$ in lieu of (or in addition to) OHC (TCHP) in TC forecasting.

Glenn et al. (2013) showed that ocean conditions similar to those on the Texas shelf during Harvey were present when Hurricane Sandy made landfall along the Mid-Atlantic Bight in October 2012. An autonomous underwater glider deployed ahead of the hurricane revealed a two-layer structure: a ~30-m surface layer of 16–17 °C and a thin, 9–10 °C bottom layer separated by a narrow thermocline. Downwelling favorable winds before Sandy forced much of this bottom water offshore. As a result, the shelf water responded as a single layer when Sandy came ashore and mixing resulted in little cooling of the surface to reduce the wind speed. Consequentially, it made landfall with greater intensity than predicted. The authors concluded by advocating for ocean observations which are essential for providing subsurface information to improve TC forecasts. We echo this sentiment. Hurricane models rely heavily on quality data to produce reliable forecast and while satellites go a long way to fulfilling this goal, they stop short. Hurricanes interact with the ocean surface but impact the water to depths where satellites become ineffective. Vigorous mixing, which redistributes heat horizontally and vertically, directly impacts storm intensity. In deep water, cooling is typical, and—to a greater or lesser extent—negatively impacts intensity. On the coasts this is not always the case. As we have seen, an unstratified, uniform water column under strong wind forcing can maintain its SST and contribute to TC intensification. There is a clear need for long-term ocean observing instruments to be deployed along the shelf of hurricane prone regions with data provided in near-real time to aid forecasting.

21699291, 2019, 4, Downloaded from https://agupubs.onlinelibrary.wiley.com/doi/10.1029/2018JC014776 by Texas A&M University Libraries Eric Hartnett, Wiley Online Library on [10/07/2025]. See the Terms and Conditions (https://onlinelibrary.wiley.com/terms-and-conditions) on Wiley Online Library for rules of use; OA articles are governed by the applicable Creative Commons License

Acknowledgments

This work was funded in part by the Texas Governors Funds, the Texas General Land Office, and the National Science Foundation under grant 1760381. Additional support was provided by the G. Unger Vetlesen Foundation. We would like to thank the captain and crew of the R/V *Manta* as well as many techs, students, and staff who participated in the cruises and were integral to the success of this research. We also thank the Gulf of Mexico Coastal Ocean Observing System (GCOOS) for hosting and disseminating the real-time data streams mentioned in this paper, which can be found at http://data.gcoos.org/. Data collected during the June and August cruises are also available through GCOOS. TABS data (http://tabs.gerg.tamu.edu/) are collected and made available through support by the Texas General Land Office; NDBC data (https://www.ndbc.noaa.gov/) are collected and made available through the U.S. Department of Commerce via NOAA. Map backgrounds provided by Google. Several color bars used follow the conventions of Thyng et al. (2016).

References

Argo (2000). Argo float data and metadata from Global Data Assembly Centre (Argo GDAC). *SEANOE.*. http://doi.org/10.17882/42182

Balaguru, K., Foltz, G. R., Leung, L. R., Hagos, S. M., & Judi, D. R. (2018). On the use of ocean dynamic temperature for hurricane intensity forecasting. *Weather and Forecasting*, *33*(2), 411–418. https://doi.org/10.1175/WAF-D-17-0143.1

Becker, R. (2017). How did Hurricane Havey get so strong? Retrieved November 6, 2018, from The Verge: https://www.theverge.com/2017/8/25/16207190/hurricane-harvey-category-four-intensity-warm-water-gulf

Bender, L. C. III, Guinasso, N. L. Jr., Walpert, J. N., Lee, L. L. III, Martin, R. D., Hetland, R. D., et al. (2007). Development, operation, and results from the Texas automated buoy system. *Gulf of Mexico Science*, *25*(1), 4.

Blake, E. S., & Zelinsky, D. A. (2018). National Hurricane Center Tropical Cyclone Report, Hurricane Harvey. Retrieved February 19, 2019 from The National Hurricane Center https://www.nhc.noaa.gov/data/tcr/AL092017_Harvey.pdf

Byers, H. R. (1959). *General Meteorology*, (p. 540). New York: McGraw-Hill.

Carrasco, C. A., Landsea, C. W., & Lin, Y. L. (2014). The influence of tropical cyclone size on its intensification. *Weather and Forecasting*, *29*(3), 582–590. https://doi.org/10.1175/WAF-D-13-00092.1

Chang, S. W. (1979). The response of an axisymmetric model tropical cyclone to local variations of sea surface temperature. *Monthly Weather Review*, *107*(6), 662–666. https://doi.org/10.1175/1520-0493(1979)107<0662:TROAAM>2.0.CO;2

CIA.gov. (2019). The World Factbook. Retrieved March, 25, 2019, from Central Intelligence Agency. Retrieved fom https://www.cia.gov/library/publications/the-world-factbook/rankorder/2233rank.html

Collins, C. O., Potter, H., Lund, B., Tamura, H., & Graber, H. C. (2018). Directional wave spectra observed during intense tropical cyclones. *Journal of Geophysical Research: Oceans*, *123*, 773–793. https://doi.org/10.1002/2017JC012943

DeMaria, M., & Kaplan, J. (1994). Sea surface temperature and the maximum intensity of Atlantic tropical cyclones. *Journal of Climate*, *7*(9), 1324–1334. https://doi.org/10.1175/1520-0442(1994)007<1324:SSTATM>2.0.CO;2

DeMaria, M., Sampson, C. R., Knaff, J. A., & Musgrave, K. D. (2014). Is tropical cyclone intensity guidance improving? *Bulletin of the American Meteorological Society*, *95*(3), 387–398. https://doi.org/10.1175/BAMS-D-12-00240.1

Demuth, J. L., DeMaria, M., & Knaff, J. A. (2006). Improvement of Advanced Microwave Sounding Unit tropical cyclone intensity and size estimation algorithms. *Journal of Applied Meteorology and Climatology*, *45*(11), 1573–1581. https://doi.org/10.1175/JAM2429.1

DiMarco, S. F., Walpert, J., Knap, A. H., Whilden, K., Lee, L. L., & Buschang, S. (2018). Coastal ocean observations during Hurricane Harvey (2017) from the Texas Automated Buoy System (TABS). [IS12A-08]. *2018 Ocean Sciences Meeting,* Portland, OR, 12–16 Feb.

Emanuel, K. A. (1986). An air-sea interaction theory for tropical cyclones. Part I: Steady-state maintenance. *Journal of the Atmospheric Sciences*, *43*(6), 585–605. https://doi.org/10.1175/1520-0469(1986)043<0585:AASITF>2.0.CO;2

Frank, W. M., & Ritchie, E. A. (2001). Effects of vertical wind shear on the intensity and structure of numerically simulated hurricanes. *Monthly Weather Review*, *129*(9), 2249–2269. https://doi.org/10.1175/1520-0493(2001)129<2249:EOVWSO>2.0.CO;2

Glenn, S., Aragon, D., Bowers, L., Crowley, M., Dunk, R., Evans, C., et al. (2013). Process-driven improvements to hurricane intensity and storm surge forecasts in the Mid-Atlantic Bight: Lessons learned from Hurricanes Irene and Sandy, In *OCEANS-Bergen,* 2013 *MTS/IEEE* (pp. 1–9). IEEE.

Gonella, J. (1972). A rotary-component method for analysing meteorological and oceanographic vector time series. *Deep Sea Research and Oceanographic Abstracts*, *19*(12), 833–846. https://doi.org/10.1016/0011-7471(72)90002-2

Goni, G., DeMaria, M., Knaff, J., Sampson, C., Ginis, I., Bringas, F., et al. (2009). Applications of satellite-derived ocean measurements to tropical cyclone intensity forecasting. *Oceanography*, *22*(3), 190–197. https://doi.org/10.5670/oceanog.2009.78

Gulf of Mexico Ocean Observing System Banner Story. (2017). Retrieved August 12, 2018, from Gulf of Mexico Coastal Ocean Observing system: http://gcoos.tamu.edu/?p=12292

Hamilton, P., Leben, R., Bower, A., Furey, H., & Pérez-Brunius, P. (2018). Hydrography of the Gulf of Mexico using autonomous floats. *Journal of Physical Oceanography*, *48*(4), 773–794. https://doi.org/10.1175/JPO-D-17-0205.1

Huang, P., Sanford, T. B., & Imberger, J. (2009). Heat and turbulent kinetic energy budgets for surface layer cooling induced by the passage of Hurricane Frances (2004). *Journal of Geophysical Research*, *114*, C12023. https://doi.org/10.1029/2009JC005603

Jaimes, B., Shay, L. K., & Brewster, J. K. (2016). Observed air-sea interactions in tropical cyclone Isaac over loop current mesoscale eddy features. *Dynamics of Atmospheres and Oceans*, *76*, 306–324. https://doi.org/10.1016/j.dynatmoce.2016.03.001

Jaimes, B., Shay, L. K., & Uhlhorn, E. W. (2015). Enthalpy and momentum fluxes during Hurricane Earl relative to underlying ocean features. *Monthly Weather Review*, *143*(1), 111–131. https://doi.org/10.1175/MWR-D-13-00277.1

Kossin, J. P., & DeMaria, M. (2016). Reducing operational hurricane intensity forecast errors during eyewall replacement cycles. *Weather and Forecasting*, *31*(2), 601–608. https://doi.org/10.1175/WAF-D-15-0123.1

Landsea, C. (2018). Atlantic Oceanic and Meteorological Laboratory. Retrieved Sept. 2018 from National Oceanic and Atmospheric Administration: http://www.aoml.noaa.gov/hrd/tcfaq/E19.html

Lee, C. Y., & Chen, S. S. (2012). Symmetric and asymmetric structures of hurricane boundary layer in coupled atmosphere–wave–ocean models and observations. *Journal of the Atmospheric Sciences*, *69*(12), 3576–3594. https://doi.org/10.1175/JAS-D-12-046.1

Leipper, D. F., & Volgenau, D. (1972). Hurricane heat potential of the Gulf of Mexico. *Journal of Physical Oceanography*, *2*(3), 218–224. https://doi.org/10.1175/1520-0485(1972)002<0218:HHPOTG>2.0.CO;2

Lin, I. I., Pun, I. F., & Wu, C. C. (2009). Upper-ocean thermal structure and the western North Pacific category 5 typhoons. Part II: Dependence on translation speed. *Monthly Weather Review*, *137*(11), 3744–3757.

Lin, I. I., Wu, C. C., Emanuel, K. A., Lee, I. H., Wu, C. R., & Pun, I. F. (2005). The interaction of Supertyphoon Maemi (2003) with a warm ocean eddy. *Monthly Weather Review*, *133*(9), 2635–2649. https://doi.org/10.1175/MWR3005.1

Mainelli, M., DeMaria, M., Shay, L. K., & Goni, G. (2008). Application of oceanic heat content estimation to operational forecasting of recent Atlantic category 5 hurricanes. *Weather and Forecasting*, *23*(1), 3–16. https://doi.org/10.1175/2007WAF2006111.1

Malkus, J. S. (1962). *Large-Scale Interactions. The Sea. Vol 1*, (pp. 86–322). New York: Wiley.

McDougall, T. J., & Barker, P. M. (2011) Getting started with TEOS-10 and the Gibbs Seawater (GSW) Oceanographic Toolbox (28 pp., SCOR/IAPSO WG127).

Mei, W., Pasquero, C., & Primeau, F. (2012). The effect of translation speed upon the intensity of tropical cyclones over the tropical ocean. *Geophysical Research Letters*, *39*, L07801. https://doi.org/10.1029/2011GL050765

Miyamoto, Y., & Takemi, T. (2010). An effective radius of the sea surface enthalpy flux for the maintenance of a tropical cyclone. *Atmospheric Science Letters*, *11*(4), 278–282. https://doi.org/10.1002/asl.292

Park, J. J., Kwon, Y. O., & Price, J. F. (2011). Argo array observation of ocean heat content changes induced by tropical cyclones in the North Pacific. *Journal of Geophysical Research*, *116*, C12025. https://doi.org/10.1029/2011JC007165

21699291, 2019, 4, Downloaded from https://agupubs.onlinelibrary.wiley.com/doi/10.1029/2018JC014776 by Texas A&M University Libraries Eric Hartnett, Wiley Online Library on [10/07/2025]. See the Terms and Conditions (https://onlinelibrary.wiley.com/terms-and-conditions) on Wiley Online Library for rules of use; OA articles are governed by the applicable Creative Commons License

Potter, H. (2018). The cold wake of Typhoon Chaba (2010). *Deep Sea Research Part I: Oceanographic Research Papers*, *140*, 136–141. https://doi.org/10.1016/j.dsr.2018.09.001

Potter, H., Drennan, W. M., & Graber, H. C. (2017). Upper ocean cooling and air-sea fluxes under typhoons: A case study. *Journal of Geophysical Research: Oceans*, *122*, 7237–7252. https://doi.org/10.1002/2017JC012954

Price, J. F. (1981). Upper ocean response to a hurricane. *Journal of Physical Oceanography*, *11*(2), 153–175. https://doi.org/10.1175/1520-0485(1981)011<0153:UORTAH>2.0.CO;2

Price, J. F. (2009). Metrics of hurricane-ocean interaction: Vertically-integrated or vertically-averaged ocean temperature? *Ocean Science*, *5*(3), 351–368. https://doi.org/10.5194/os-5-351-2009

Schade, L. R., & Emanuel, K. A. (1999). The ocean's effect on the intensity of tropical cyclones: Results from a simple coupled atmosphere–ocean model. *Journal of the Atmospheric Sciences*, *56*(4), 642–651. https://doi.org/10.1175/1520-0469(1999)056<0642:TOSEOT>2.0.CO;2

Shay, L. K. (2006). Positive feedback regimes during tropical cyclone passage. Preprints, 14th Conf. on the Interaction of the Sea and the Air, Atlanta, GA, Amer. Meteor. Soc., *10*.7

Shay, L. K., Goni, G. J., & Black, P. G. (2000). Effects of a warm oceanic feature on Hurricane Opal. *Monthly Weather Review*, *128*(5), 1366–1383. https://doi.org/10.1175/1520-0493(2000)128<1366:EOAWOF>2.0.CO;2

Shen, W., & Ginis, I. (2001). The impact of ocean coupling on hurricanes during landfall. *Geophysical Research Letters*, *28*(14), 2839–2842. https://doi.org/10.1029/2001GL013151

Sitkowski, M., Kossin, J. P., & Rozoff, C. M. (2011). Intensity and structure changes during hurricane eyewall replacement cycles. *Monthly Weather Review*, *139*(12), 3829–3847. https://doi.org/10.1175/MWR-D-11-00034.1

Thyng, K. M., Greene, C. A., Hetland, R. D., Zimmerle, H. M., & DiMarco, S. F. (2016). True colors of oceanography. *Oceanography*, *29*(3), 10.

Trenberth, K. E., Cheng, L., Jacobs, P., Zhang, Y., & Fasullo, J. (2018). Hurricane Harvey links to ocean heat content and climate change adaptation. *Earth's Future*, *6*(5), 730–744. https://doi.org/10.1029/2018EF000825

Wang, X., Wang, X., & Chu, P. C. (2018). Air-sea interactions during rapid intensification of typhoon Fengshen (2008). *Deep Sea Research Part I: Oceanographic Research Papers*, *140*, 63–77. https://doi.org/10.1016/j.dsr.2018.08.009

Weatherford, C. L., & Gray, W. M. (1988). Typhoon structure as revealed by aircraft reconnaissance. Part II: Structural variability. *Monthly Weather Review*, *116*(5), 1044–1056. https://doi.org/10.1175/1520-0493(1988)116<1044:TSARBA>2.0.CO;2

Weisman, M. L., & Klemp, J. B. (1982). The dependence of numerically simulated convective storms on vertical wind shear and buoyancy. *Monthly Weather Review*, *110*(6), 504–520. https://doi.org/10.1175/1520-0493(1982)110<0504:TDONSC>2.0.CO;2

Whitaker, W. D. (1967). Quantitative determination of heat transfer from sea to air during passage of hurricane Betsy (Doctoral Dissertation, Texas A&M University).

Wright, C. W., Walsh, E. J., Vandemark, D., Krabill, W. B., Garcia, A. W., Houston, S. H., et al. (2001). Hurricane directional wave spectrum spatial variation in the open ocean. *Journal of Physical Oceanography*, *31*(8), 2472–2488. https://doi.org/10.1175/1520-0485(2001)031<2472:HDWSSV>2.0.CO;2

Xu, J., & Wang, Y. (2010). Sensitivity of tropical cyclone inner-core size and intensity to the radial distribution of surface entropy flux. *Journal of the Atmospheric Sciences*, *67*(6), 1831–1852. https://doi.org/10.1175/2010JAS3387.1

21699291, 2019, 4, Downloaded from https://agupubs.onlinelibrary.wiley.com/doi/10.1029/2018JC014776 by Texas A&M University Libraries Eric Hartnett, Wiley Online Library on [10/07/2025]. See the Terms and Conditions (https://onlinelibrary.wiley.com/terms-and-conditions) on Wiley Online Library for rules of use; OA articles are governed by the applicable Creative Commons License